JOURNAL OF MATERIALS SCIENCE: MATERIALS IN MEDICINE **10** (1999) 663–670

Quantification of bone ingrowth within bone-derived porous hydroxyapatite implants of varying density

K. A. HING, S. M. BEST, K. E. TANNER, W. BONFIELD
IRC in Biomedical Materials, Queen Mary and Westfield College, Mile End Road, London E1 4NS, UK

P. A. REVELL
IRC in Biomedical Materials, Royal Free Hospital School of Medicine, Rowland Hill Street, London NW3, UK

Hydroxyapatite has been investigated for use in the osseous environment for over 20 years and the biocompatibility of the ceramic and its osseoconductive behavior is well established. Therefore, the use of porous hydroxyapatite for the repair of osseous defects seems promising with potential for complete penetration of osseous tissue and restoration of vascularity throughout the repair site. However, there have been few systematic studies of the effects of physical properties such as macropore size and pore connectivity on the rate and quality of bone integration within porous hydroxyapatite implants. This paper quantifies the early biological response to a well-characterized series of implants with uniform microstructure and phase composition, but differing macrostructures and demonstrates the dependence of the rate of osseointegration on the apparent density of porous hydroxyapatite as a function of pore connectivity. Furthermore, compression testing established that bony ingrowth has a strong reinforcing effect on porous hydroxyapatite implants, which is more pronounced in the lower density implants, as a result of a greater relative volume of bone ingrowth.

1. Introduction

The biocompatibility [1–3] of hydroxyapatite ($Ca_{10}(PO_4)_6(OH)_2$) and the similarities between the crystal structure of hydroxyapatite (HA) and bone mineral [4, 5] has led to great interest in the potential of dense HA as a material for the augmentation of osseous defects. The use of low density HA, with highly interconnected porosity, has also been advocated as a viable alternative to bone grafts without the complications of sterilization, infection, rejection and inadequate supply. Furthermore, porous structures invite ingrowth of bone into the implant, leading to a more securely fixed and integrated repair, particularly in cancellous bone where the structure closely mirrors that of the host.

Ideally, porous implants should induce a response similar to that of fracture healing, when placed in an osseous defect [6], where the implant porosity is initially invaded by mesenchymal cells, fibroblasts and osteoblasts, before new trabeculae of bone infiltrate into the porous structure from the walls of the defect. Then, once the implant is fully integrated, the new bone should be remodeled into a more organized (lamellar) bone structure. This sequence of events has been reported in a number of previous investigations [7–11], but the timing of events vary, i.e. bone integration was reported to be retarded in coralline-derived porous hydroxyapatites implants, relative to defects repaired with bone grafts [11]. In contrast, the direct apposition of lamellar bone has been reported [12] within the porous structure of osseointegrated porous hydroxyapatites manufactured from synthetic HA. Furthermore, it has been reported [13] that fibrous tissue can invade and colonize faster than osseous tissue, so inhibiting later bone deposition. These variations highlight the importance of systematic histological studies at early time points, and the value of information regarding the early histological response of a material in aiding the understanding of longer-term behavior.

The morphology of ceramic implants has been considered since the use of porous materials were first described in 1963 [14]. Moreover, Hulbert *et al.* [15] demonstrated that porous discs of a near-inert ceramic exhibited thinner fibrous encapsulation with faster healing in surrounding muscle and connective tissue when compared with dense discs of the same composition implanted in the same site. The authors postulated that this resulted from mechanical interlock, which reduced motion between host tissue and implant, eliciting a more passive response from the host. However, there still seems to be some dispute regarding the optimum ''type'' of porosity, perhaps as a result of inadequate characterization of morphology and a lack of consideration regarding the possibility of different ''optimum'' structures for materials with different

levels of biocompatibility. A minimum pore size of 100–135 μm for sustained healthy bone ingrowth in polyethylene has been established [16] and this figure is often cited for both metallic and ceramic structures. However, while many studies have considered the effect of pore morphology upon osseointegration [7, 8, 10, 11, 15–20], little or no quantification of bone ingrowth or pore structure has been reported, and systematic measurement of the mineral apposition rate within porous implants is rare. Generally, the majority of investigations into the osseointegration of porous HA have reported an increase in the volume of bone ingrowth with increasing pore size, and many authors have concluded that this reflects a dependence of bone ingrowth on the pore size [7, 8, 17–19]. However, some authors [11, 20] have challenged this perspective and suggest that it is an increase in the size and frequency of pore interconnections, or connectivity, that has resulted in a greater penetration of bone ingrowth within porous implants, especially at early time points. However, as connectivity generally increases with increasing pore size, separating the contributions of the two parameters on the volume of bone ingrowth is not a trivial problem. If one considers how the two parameters may influence the volume of bone ingrowth, then it is clear that variations in pore size will control bone ingrowth as a function of available space for occupation. Therefore, if the volume percentage of bone ingrowth were normalized to pore volume then the normalized values for bone ingrowth within different pore structures should be equivalent. In contrast, connectivity will control the frequency of pathways for osteogenic cells and nutrients to enter the porous structure, and therefore the rate of bone integration, leading to greater volumes of bone within more open structures, particularly at early time points. Thus measurement of both the normalized volume of bone ingrowth and the rate of integration should identify which parameter dominates osseointegration within a porous structure. Furthermore, earlier work [21–23] has demonstrated that the characteristics of porosity strongly effect the mechanical behavior of ceramic foams, with compressive modulus and ultimate compressive strength being highly sensitive to both density and pore isotropy. Thus, given that pore connectivity is maintained, implants with larger pore sizes will inherently be weaker as a result of an associated reduction in density. Therefore, knowledge regarding the change in strength resulting from ingrowth related reinforcement, as a function of changes in implant density would be useful when selecting material for different surgical applications. Previously, compression testing has been successfully employed in the evaluation of the mechanical properties of cancellous bone and candidate synthetic bone materials [8, 10, 24]. Where implant compressive strength was measured both before and after implantation, these investigations demonstrated bone ingrowth to have a strong reinforcing effect on porous HA implants. An increase from 4 to 25 MPa in ultimate compressive strength was reported for coralline porous HA after 6 months *in vivo* [8], while the compressive strength of porous HA derived from cancellous bone was found to increase from 2 to 20 MPa after 3 months *in vivo* [23]. Furthermore, the compressive strength of blocks of porous HA/tri-calcium phosphate composites increased from 3 to 6 MPa after only 1 week *in vivo* [24]. However, few comprehensive studies on the reinforcing effect of bone ingrowth within porous implants with systematically varying apparent densities have been reported.

Therefore, this paper aims to quantify the magnitude and rate of early bone ingrowth within three batches of porous HA as a function of differing macrostructure, by measurement of both the absolute and normalized percentage of bone ingrowth, and measurement of the mineral apposition rate of bone within the porous structure of the implants. Furthermore, in addition to quantification of the bone ingrowth, an assessment of the effect of bone ingrowth on the overall mechanical behavior of the osseointegrated implants has been made.

2. Methods

2.1. Implant materials

Three well-characterized batches of porous HA (Endobon®, E. Merck GmbH)) with uniform microstructure and phase composition, but differing macrostructure, were selected for implantation. The full chemical, physical and mechanical characterization of these implants has previously been reported [25] and the salient points of the physical and mechanical characterization are summarized in Table I. Endobon® is a derivative of natural cancellous bone, produced via the hydrothermal conversion of bovine cancellous bone to ceramic hydroxyapatite. Material was supplied in the form of cylindrical specimens with a mean diameter of 4.58 ± 0.07 mm and a mean length of 6.56 ± 0.40 mm. The three batches of specimens possessed mean apparent densities of 1.23 ± 0.05, 0.90 ± 0.04 and 0.60 ± 0.04 g cm^{-3}, and were designated as batches A, C and B, respectively.

TABLE I Physical and mechanical characteristics of Batches A, B and C

Batch	Pore length (μm)		Pore breadth (μm)		Connectivity indicator	Ultimate compressive stress (MPa)	Compressive modulus (GPa)
	Mean	Mode	Mean	Mode			
A	390 [480]	500	310 [120]	350	0.8 [0.5]	9.4 [1.7]	1.4 [0.4]
C	790 [420]	750	450 [220]	400	1.2 [0.9]	5.6 [0.9]	0.9 [0.3]
B	1360 [680]	1500	640 [290]	550	2.4 [1.2]	2.2 [0.9]	0.7 [0.4]

2.2. Implantation procedure

All implantations were carried out on 6 month New Zealand White rabbits of mixed sex. Implants were placed in the distal condyle of the right femur. This site was selected as it presented the largest volume of load bearing cancellous bone within the animal. A hole approximately 6 mm in depth was drilled using a 4.5 mm external diameter, diamond-tipped trephine and a compressed-air powered drill. During drilling, sterile saline was fed through the drill and the hole depth was monitored using millimeter graduations on the side of the trephine. Specimens were press fitted into the defect and the site was washed with sterile saline before both the joint capsule and skin incisions were closed with interrupted PDS monofilament and Vicryl sutures, respectively. After operation animals were isolated in a recovery room overnight. They were subsequently kept in open pens in groups of five to six and allowed full use of the knee. Rabbits selected for labeling were injected subcutaneously on three consecutive days of each designated week (Table II). For histological assessment of early reparative processes only low density (Batch B) specimens were retrieved after 10 days *in vivo*. Additional Batch B implants and implants from the other two batches were retrieved after a period of 5 weeks. Rabbits were sacrificed by injecting an overdose of anaesthetic (Hyprorm/Diazepam). The appearance of surrounding tissue, the extent of healing undergone at the site of implantation, the mobility of the joint and any other abnormalities were noted. After termination, the distal end of the operated femur was completely removed and all soft tissue was stripped from the bone.

2.3. Histological evaluation and histomorphometry

All dissected femora designated for microscopy, fluorochrome labeled and unlabeled, were trimmed and placed immediately in formal alcohol fixative (comprising 70% ethanol) for a period of 4 days. The fixed tissue was dehydrated and embedded in Technovit resin. The resin blocks were then processed through to semithin (5–10 μm) sections using the Exakt technique [26]. Sections for histological examination were stained with Toluidine blue, while those prepared for fluorescence microscopy were mounted unstained.

Histomorphometry was performed using point counting and linear intercept techniques. The percentage of bony ingrowth was measured using a Weibel grid composed of 42 points [27]. Measurements were made on longitudinally sectioned specimens split into nine measurement zones. Measurement of the total area occupied by bone ingrowth, HA and pore space within each zone was made to determine the bone, strut and pore volumes, respectively, for each specimen. Thus, by determination of both the pore volume available for osseointegration and the volume occupied by bone ingrowth within each specimen, both the absolute and normalized percentages of bone ingrowth within the pore space, for each implant, were calculated using Equations 1 and 2

$$\text{Absolute volume of bone ingrowth, } VB_A(\%) = \frac{\text{Bone Volume}}{\text{Implant (strut + pore) volume}} \times 100 \quad (1)$$

$$\text{Normalized volume of bone ingrowth, } VB_N(\%) = \frac{\text{Bone volume}}{\text{Pore volume}} \times 100 \quad (2)$$

The mineral apposition rate (MAR) of bone ingrowth between weeks 2–3 and 3–4, within porous HA implants was determined using Equation 3 [28]

$$\text{Mineral apposition rate, MAR } (\mu\text{m day}^{-1}) = \frac{0.74 \sum_{x=1}^{x=n} D_x}{n \times t}$$

Where D is the measured distance between two fluorochrome labels, in μm, n is the number of measurements and t the time interval between administration of the fluorochrome labels, in days. Determination of the apposition rates of bone deposited between weeks 1–2 was not possible as a result of the predominance of woven bone and the convoluted nature of the bone seams laid down during this time period. As a control, the MAR of cancellous bone in the apposition phase of the remodeling cycle, at a distance of 2 mm from the defect site, was also determined.

2.4. Compression testing

The extent of reinforcement was assessed by compression testing of cylindrical plugs, trephined from retrieved femora, such that each test piece was composed of an intact implant with its associated bone ingrowth. Compression testing was carried out using an Instron 4464 bench top test machine fitted with a 2 kN load cell and an environmental chamber which allowed the test to be performed in Ringer's solution at 37 °C while load

TABLE II Fluorochrome labeling protocols

Label	Concentration (mg ml^{-1})	Dosage (mg kg^{-1})	Days injected after operation	
			Batch B	Batch A and C
Tetracycline	20	0.5	6,7,8	13,14,15
Calcein Blue	50	0.2	14,15,16	–
Alizarin Red	30	0.5	21,22,23	–
Calcein Green	30	0.5	28,29,30	20,21,22

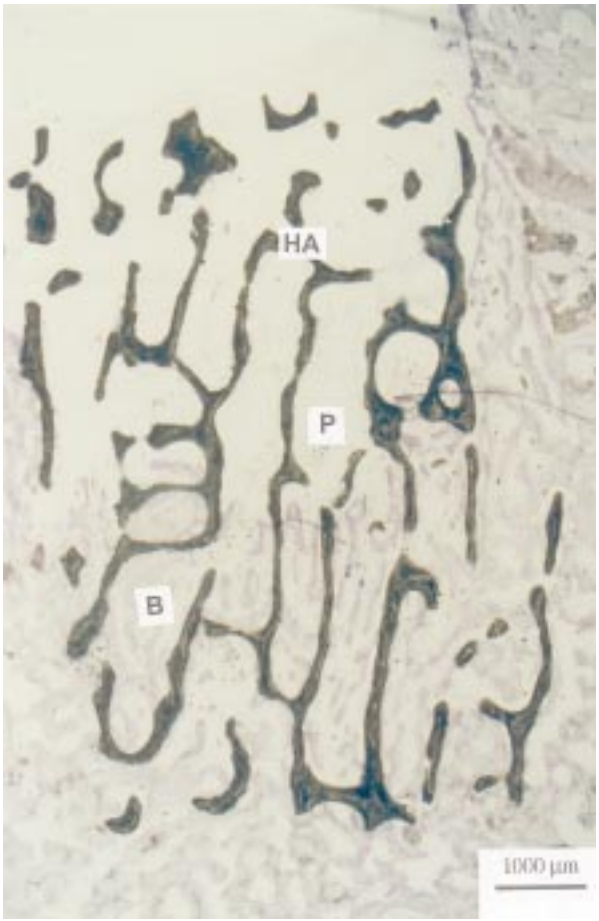

Figure 1 Infiltration of bone ingrowth from the deep end of the defect within a Batch B implant. (HA, Hydroxyapatite; B, new bone; P, pore space).

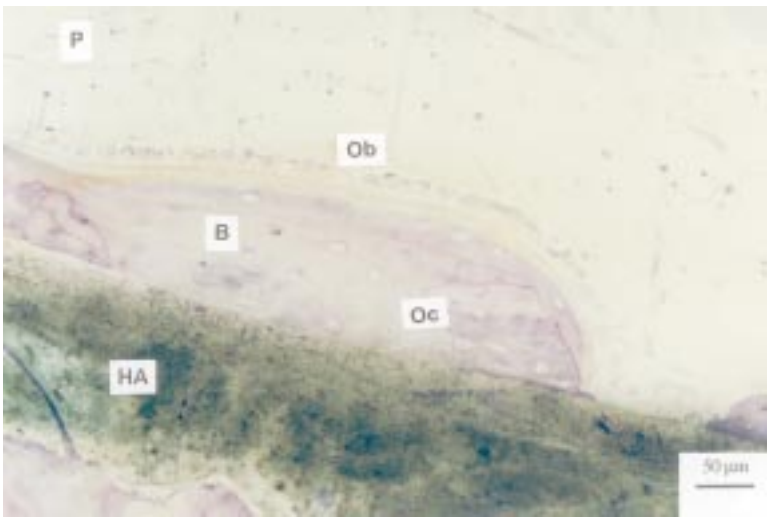

Figure 2 Direct apposition of bone on an internal pore surface. HA, Hydroxyapatite; B, new bone; Oc, osteocytes; Ob, osteoblasts; P, pore space.

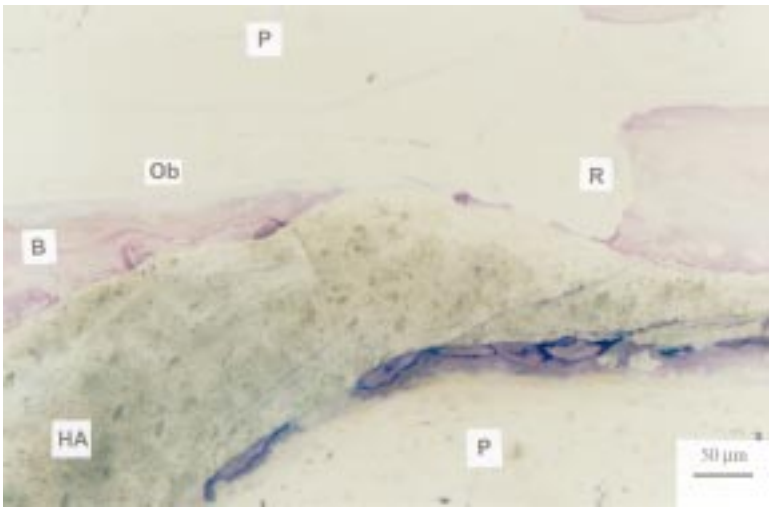

Figure 3 Remodeling of bone around a HA strut. HA, Hydroxyapatite; B, new bone; Ob, osteoblasts; R, resorption front; P, pore space.

(a)

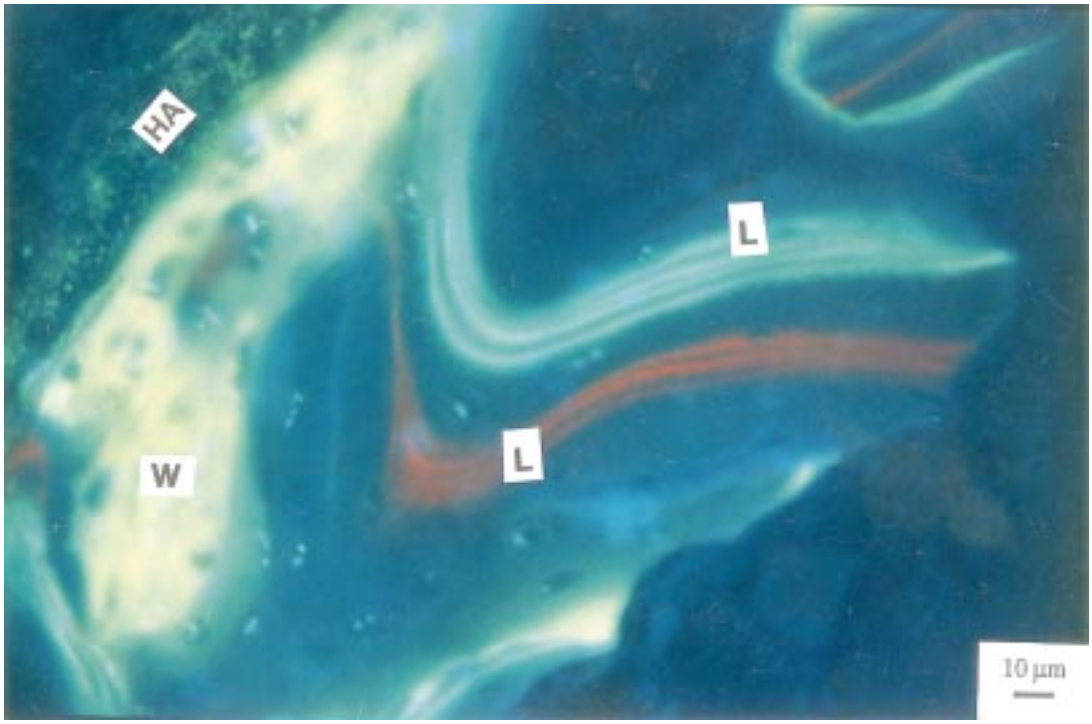

(b)

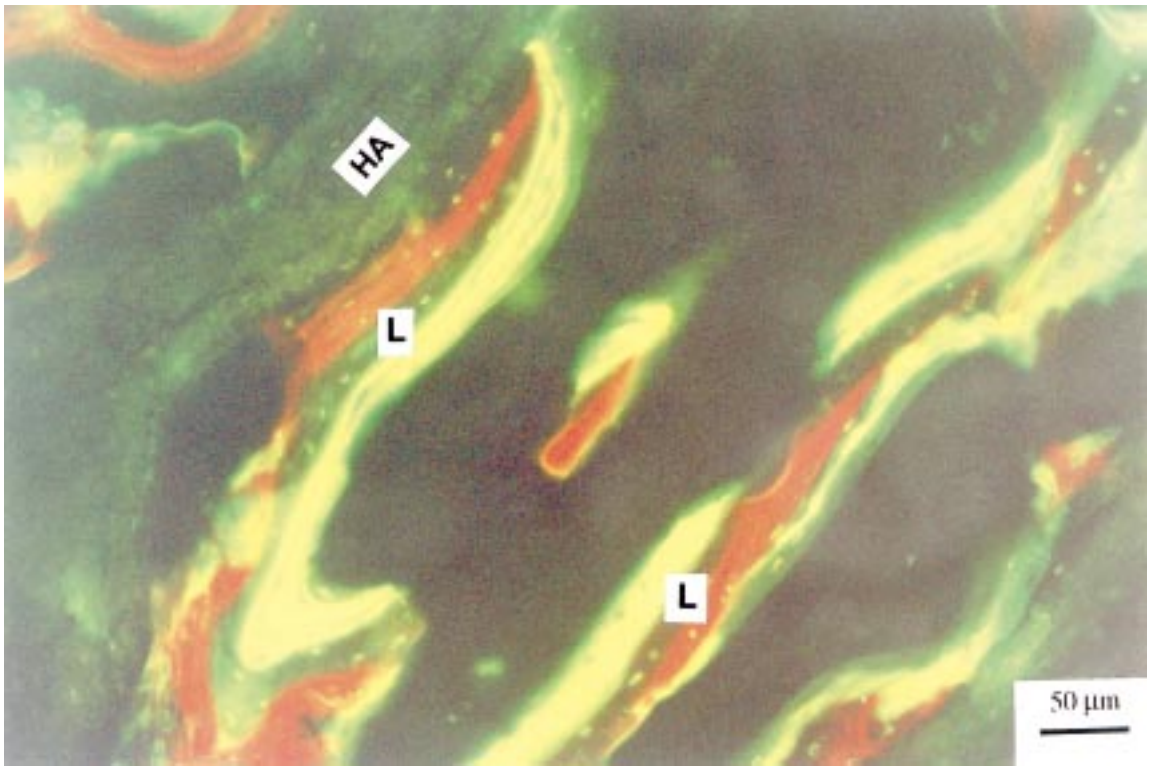

Figure 4 (a) Fluorochrome labeled woven (W) and lamellar (L) bone at the periphery of an implant. (b) Fluorochrome labelled lamelar (L) bone within the porosity of an implant.

was applied axially to the specimens with a crosshead velocity of 0.1 mm min^{-1}.

3. Results

3.1. Histological evaluation

There was no evidence of bone regeneration within the center of the macroporous structure of the implant and only isolated areas of bone regeneration in the periphery of implants after 10 days *in vivo*. The site appeared to be recovering from the surgical procedure, with significant regeneration of bone occurring from the deep end of the defect and limited regeneration occurring at the defect walls. The interior of the implant contained a mixture of clotted blood and assorted cells. There was no conclusive evidence of osseoinductive behavior at this time point, as the isolated instances of regeneration in the periphery of the implant may have been due to osseoconduction from the surrounding bone. Extensive osseointegration was noted at 5 weeks in all batches of implant, with seams of osteoblasts depositing bone directly on the implant surfaces and the primary direction of bone ingrowth occurring from the deep end towards the superficial end of the defect, with some integration from the walls (Fig. 1). However, the depth of penetration was reduced in the higher density specimens (batches C and A). The histological response to implants of all densities (batches B, C and A) after 5 weeks *in vivo* was similar. Fibrous encapsulation was not observed around the implants and there was evidence of the direct apposition of bone on internal pore surfaces, with osteocytes in close proximity to the implant material (Fig. 2). Active areas of bone deposition, characterized by seams of cuboidal, darkly stained osteoblasts, resorption and remodeling (Fig. 3) occurred within all implants. There was also some evidence of tissue integration within the ceramic struts. From the fluorochrome labeling, it was evident that bone at the periphery of the implant was rapidly laid woven bone, and any bone observed within the implant macropores (usually near the periphery) that had been deposited within the first 2 weeks was also woven in nature (Fig. 4a). However, the direct apposition of lamellar bone was observed on central, internal strut surfaces at 2, 3 and 4 weeks (Fig. 4b). The chronological ordering of the labels, from the implant surface to the bone surface, also demonstrated that the majority of ingrowth within the implants commenced at the strut surfaces and grew into the macropores, suggesting osseoinductive behavior.

3.2. Histomorphometry

Histomorphometric analysis demonstrated that, after 5 weeks *in vivo*, the absolute volume of bone ingrowth within a porous HA implant increased from 10 to 24% of the implant volume, as the apparent density decreased (Fig. 5a). Moreover, this trend was also true for the normalized data (increasing from 24 to 32% of the pore volume) indicating that the reduction in bone ingrowth in higher density implants was not entirely due to the differences in pore size, at this time point (Fig. 5b).

Mineral apposition rates (MAR) calculated for bone ingrowth within all batches of porous HA during weeks 2–3 and 3–4 were found to vary, where the MAR of low density (Batch B) and medium density (Batch C) implants were somewhat elevated (3.8 μm day^{-1} and 3.4 μm day^{-1}, respectively) compared to the MAR of control bone (3.1 μm day^{-1}). In contrast, the MAR of bone ingrowth within the high density implants was reduced to 2.8 μm day^{-1} (Table III). These results confirm the histomorphometric observations that the volume of ingrowth was not solely dependent on the pore volume.

3.3. Compression testing

The mechanical behavior of porous HA implants in compression was found to alter on implantation (Fig. 6). Before implantation specimens failed in the manner of an elastic–brittle foam. However, after implantation for 5 weeks the failure behavior was more similar to that of cancellous bone, i.e. elastic–plastic behavior, even for

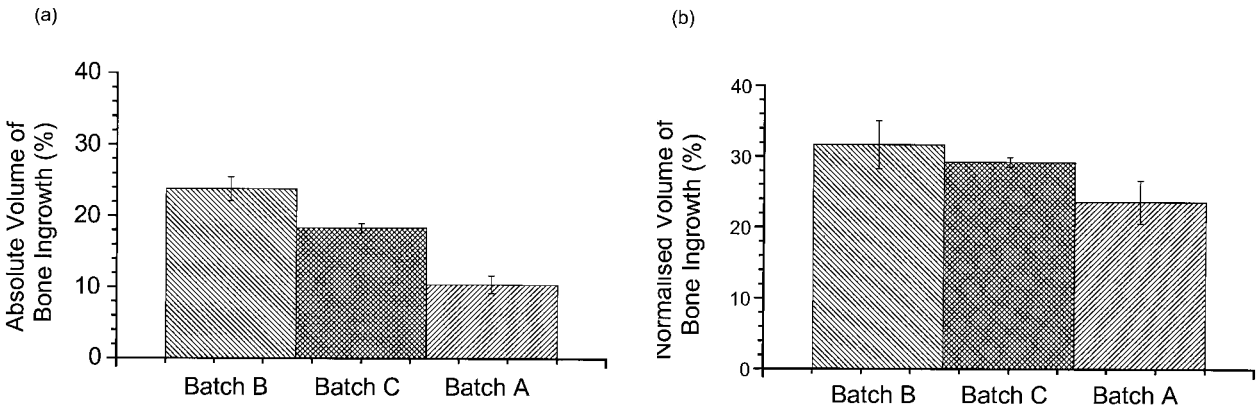

Figure 5 (a) Absolute volume of bone ingrowth (%) within the porosity of Batch B, C and A implants. (b) Normalized volume of bone ingrowth (%) within the porosity of Batch B, C and A implants.

TABLE III Mineral apposition rates (μm day^{-1}) of bone ingrowth

Control bone	Batch B	Batch C	Batch A
3.1 [0.2]	3.8 [0.3]	3.4 [0.2]	2.8 [0.2]

the higher density Batch A implants. Furthermore, the bone ingrowth was found to significantly enhance the compressive strength of all batches of implants after 5 weeks *in vivo*, despite incomplete osseointegration at this time point, (Fig. 7). This reinforcing effect was particularly pronounced for the low density implants, with a 195% increase in compressive strength whereas increases of only 70 and 20% were achieved for Batches C and A, respectively.

4. Discussion

The sequence of events observed within the Endobon® implants was similar for all batches of implant, i.e., accelerated when compared to the fracture healing response described for the repair of unfilled cavities in the rabbit femoral condyle. At 10 days the macropores were filled with blood clot and mesenchymal cells, with some bone regeneration occurring at the edges of the defect, while at 5 weeks extensive penetration of lamellar bone ingrowth was noted within the Endobon® implants. However, two distinct sequences of osseointegration were observed in the Endobon®. Observations from the 10-day time point indicated that bulk implants were intially osseoconductive, with bone ongrowth observed initiating from the defect walls towards the center of the implant. Fluorochrome labeling demonstrated that this bone was woven (Fig. 4a), indicating accelerated deposition at the periphery of the implant. This result suggests that the primary purpose of the new bone is rapid fixation of the implant (as in the encapsulation of bone ends by callus in a fracture [29]). After this initial period, once bone ongrowth and fixation had occurred, the Endobon® appeared to induce the deposition of more ordered lamellar bone on its internal surfaces and within its pores (Fig. 4b), thereby acting as a support for new bone and encouraging bone growth on its surfaces. The chronological order of labeled bone deposited on the internal macropore surfaces, from strut to bone surface indicated osseoinductive behavior within the internal macrostructure. This spontaneous deposition of bone appeared to advance from the deep end of the defect, i.e. from the most abundant source of potentially osteogenic cells. This is in contrast to the response of coralline porous HA implants implanted in the same site, where only osteoid production was reported at 6 weeks [11]. Furthermore, the bony ingrowth reported within larger coralline porous HA implants implanted in dogs remained woven until remodeling occurred between 2 and 4 months [8].

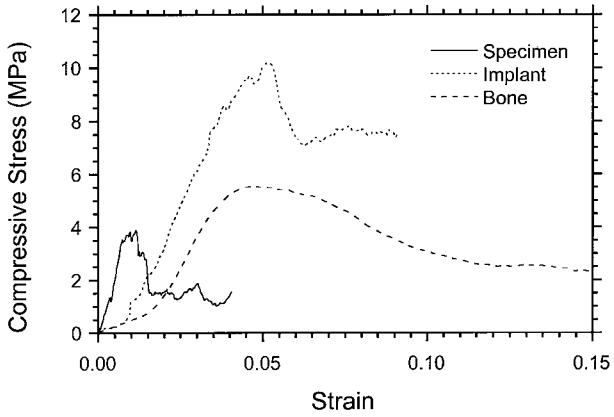

Figure 6 Typical compressive stress-strain behavior for a Batch C Specimen (Specimen), a retrieved Batch C Implant (Implant) and cancellous bone (Bone) from the same anatomical site.

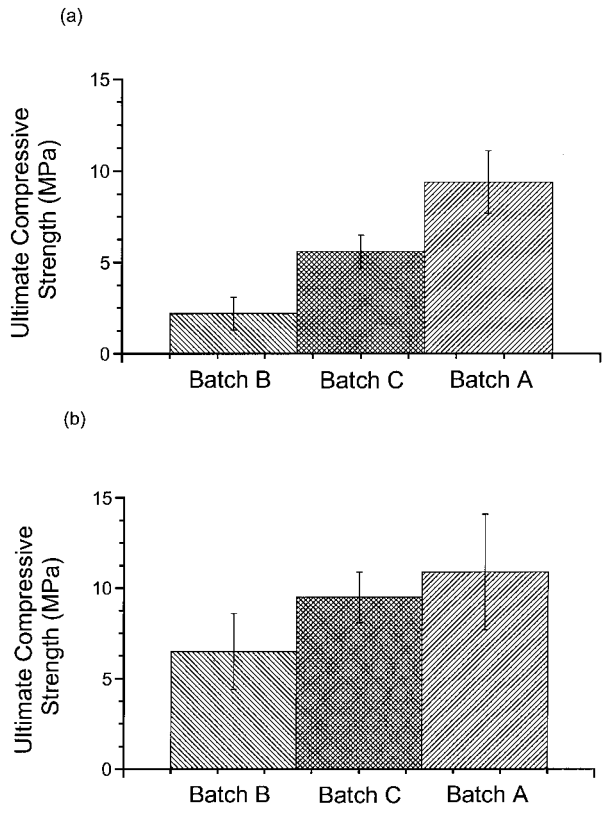

Figure 7 **(a)** Mean ultimate compressive strengths of Batch B, C and A specimens before implantation. **(b)** Mean ultimate compressive strengths of Batch B, C and A implants after 5 weeks *in vivo*.

From the results of this study it is clear that osseointegration is strongly affected by the morphology of the porous structure (Fig. 5). If considering the variation in the absolute percentage of ingrowth alone, then it appears that the degree of bone ingrowth is dependent on pore size, as has been previously reported. However, variation in the normalized ingrowth data, in conjunction with variation in the mineral apposition rate of bone ingrowth within the various batches of porous implant (Table III), conclusively demonstrated that the volume of bone ingrowth at this time point was dependent on the structure as a function of the pore connectivity. Thus at ''early'' time points, the volume of bone ingrowth is controlled primarily by morphology, i.e. as a function of the speed with which osteogenic cells can invade the structure. This variation in osseointegration rate was also highlighted by the decrease in the depth of penetration of bony ingrowth from the deep end of the implant, within the higher density implants.

The implantation of porous HA was found to have a profound effect on the mechanical behavior of the material. Before implantation specimens would fail in the manner of an elastic–brittle foam (Fig. 6), as previously described [21, 22]. However, after implantation for 5 weeks, the failure behavior was altered to one more similar to that of cancellous bone (Fig. 6), even for the higher density Batch A implants. This change in mechanical behavior indicated that the integrated implant was behaving in a similar manner to a bone-

reinforced porous HA composite, an observation corroborated by the increase in ultimate compressive strength for all batches of implant (Fig. 7). Furthermore, reduction in the level of reinforcement as implant density increased, from 195 to 20%, reflected the reduced volume of bone ingrowth in the higher density implants. A previous study into the osseointegration of bone-derived porous HA demonstrated that after 3 months *in vivo* batch B implants attained a compressive strength of approximately 15–20 MPa [23]. Similar findings were reported for coralline porous HA implants [8] (with increases in compressive strength from 4 to 25 MPa after 6 months *in vivo*), and blocks of porous tri-calcium phosphate composites [24] (where compressive strength increased from 3 to 6 MPa after 1 week *in vivo*). These results indicate, that with time, the mechanical behavior of osseointegrated implants may become independent of the initial implant strength as a result of reinforcement by bone ingrowth.

5. Conclusions

The dependence of the rate of osseointegration on the apparent density of porous HA as a function of pore connectivity has been demonstrated. This dependence was found to be caused by a reduction in the rate of bone ingrowth within the higher density specimens. The results of compression testing established that bony ingrowth has a strong reinforcing effect on porous implants, which is more pronounced in lower density implants as a result of a greater relative volume of bone ingrowth.

We therefore conclude that, despite inferior mechanical properties before implantation, lower-density porous HA presents a better implant material for the filling of osseous defects as a result of a faster rate of osseointegration leading to enhanced mechanical performance *in vivo* because of reinforcement by bone ingrowth. However, one must also consider that the implant must survive handling and surgical procedure intact, as loss of the integrity of the open porous structure may retard osseointegration, and hence fixation and reinforcement, as a function of apparent structural densification. Thus, an optimum balance between porosity and strength must be attained. Confirmation of this hypothesis, i.e. that the volume of bone ingrowth at ''early'' time points is primarily pore interconnectivity dependent, could be obtained by comparison of the normalized volume of bone ingrowth at later time points in Batch A and B implants.

Acknowledgments

The authors gratefully acknowledge the Engineering and Physical Sciences Research Council (UK) for the core grant funding of the IRC in Biomedical Materials, and the support of E. Merck (Germany).

References

1. H. W. DENISSEN, K. DE GROOT, A. A. DRIESSEN, J. G. C. WOLKE, J. G. J. PEELEN, H. J. A. VAN DIJK, A. P. GEHRING and P. J. KLOPPER, *Sci. Ceram.* **10** (1980) 63.
2. H. AOKI, in ''Science and medical applications of hydroxyapatite'' (Takayama Press, Tokyo, 1991) 137.
3. P. K. STEPHENSON, M. A. R. FREEMAN, P. A. REVELL, J. GERMAN, M. TUKE and C. J. PIRIE, *J. Arthroplasty* **6** (1991) 51.
4. W. F. DE JONG, *Rec. Trav. Chim.* **45** (1926) 445.
5. A. S. POSNER, *Phys. Rev.* **49** (1969) 760.
6. G. HEIMKE, in ''Osseo-intergrated implants'', edited by G. Heimke (CRC Press, Boca Raton, 1990) p. 2.
7. R. E. HOLMES, *Plast. Reconstr. Surg.* **63** (1979) 626.
8. R. E. HOLMES, V. MOONEY, R. BUCHOLZ and A. TENCER, *Clin. Orthop. Rel. Res.* **188** (1984) 252.
9. F.-H. LIN, C.-C. LIN, H.-C. LIU, Y.-Y. HUANG, C.-Y. WANG and C.-M. LU, *Biomaterials* **15** (1994) 1087.
10. R. B. MARTIN, M. W. CHAPMAN, N. A. SHARKEY, S. L. ZISSIMOS and B. BAY, *ibid.* **14** (1993) 341.
11. J. H. KÜHNE, R. BARTL, B. FRISH, C. HANMER, V. JANSSON and M. ZIMMER, *Acta Orthop. Scand.* **65** (1994) 246.
12. W. RENOOIJ, H. A. HOOGENDOORN, W. J. VISSER, R. H. F. LENTFERINK, M. G. J. SCHMITZ, H. VAN IEPEREN, S. J. OLDENBURG, W. M. JANSSEN, L. M. A. AKKERMANS and P. WITTEBOL, *Clin. Orthop. Rel. Res.* **197** (1985) 272.
13. M. OGISO, Y. YAMASHITA, T. TABATA, R. RAMONITO and D. BORGESE, *J. Biomed. Mater. Res.* **28** (1994) 805.
14. J. W. SMITH, *J. Bone Joint Surg.* **45-B** (1963) 761.
15. S. F. HULBERT, J. S. MORRISON and J. J. KLAWITTER, *J. Biomed. Mater. Res.* **6** (1972) 347.
16. J. J. KLAWITTER, J. G. BAGWELL, A. M. WEINSTEIN, B. W. SAUER and J. R. PRUITT, *ibid.* **10** (1976) 311.
17. J. J. KLAWITTER and S. F. HULBERT, *ibid.* **5** (1971) 161.
18. A. UCHIDA, S. M. L. NADE, E. R. MC CARTNEY and W. CHING, *J. Bone Joint Surg.* **66-B** (1984) 269.
19. G. DACULSI and N. PASSUTI, *Biomaterials* **11** (1990) 86.
20. P. S. EGGLI, W. MULLER and R. K. SCHENK, *Clin. Orthop. Rel. Res.* **232** (1988) 127.
21. L. J. GIBSON, *J. Biomech.* **18** (1985) 317.
22. L. J. GIBSON and M. F. ASHBY, in ''Cellular solids'' (Pergamon Press, Oxford, 1988) p. 120.
23. K. A. HING, S. M. BEST, P. A. REVELL, K. E. TANNER and W. BONFIELD, *J. Mater. Sci.: Mater. Med.* **8** (1997) 731.
24. M. TRÉCANT, J. DELÉCRIN, J. ROYER, E. GOYENVALLE and G. DACULSI, *Clin. Mater.* **15** (1994) 233.
25. K. A. HING, S. M. BEST and W. BONFIELD, *J. Mater. Sci.: Mater. Med.* (in press).
26. K. DONATH, *J. Oral Pathol.* **11** (1982) 318.
27. E. R. WEIBEL and H. E. ELIAS, in ''Quantitative methods in morphology'', edited by E. R. Weibel and H. E. Elias (Springer-Verlag, Berlin, 1967) 87.
28. H. M. FROST, in ''Bone histomorphometry'', edited by P. J. Meunier (1976) 361.
29. G. H. BOURNE, in ''The biochemistry and physiology of bone'' (Academic Press, New York, 1972) p. 1.

Received 1 December 1998
and accepted 18 February 1999